In-body Path Loss Model for Homogeneous and Heterogeneous Human Tissues

Luc Martens, Divya Kurup, Wout Joseph and Gunter Vermeeren
IBBT-Ghent University, Dept. of Information Technology
Gaston Crommenlaan 8 Box 201, B-9050 Ghent, Belgium
Email: Luc.Martens@intec.UGent.be

Abstract

An in-body path loss model in homogeneous human tissues is proposed based on 3D electromagnetic simulations and validated with measurements. Simulations are further extended for different relative permittivity and conductivity combinations spanning a range of human tissues at 2.45GHz, and the influence of the dielectric properties on path loss is investigated and modeled. Finally, path loss in homogeneous medium is compared with the path loss in a heterogeneous human phantom.

1. Introduction

A wireless body area network (WBAN) is a network, consisting of nodes that communicate wirelessly and are located on or in the body of a person. A path loss (PL) model helps to design optimal communication between such nodes. Applications of WBANs include medicine, sports, and multimedia which make use of the freedom of movement provided by the WBAN. The proposed model can be used by manufacturers to evaluate the performance of in-body WBAN systems using well specified setups and to carry out link budget calculations. The goal of this paper is to develop an empirical PL model for various homogeneous human tissues and describe the relationship between the PL, the relative permittivity ε_r and the conductivity σ of the human tissues, and the distance between the antennas. Simulations and measurements are performed at 2.457 GHz in the license free industrial, scientific and medical (ISM) band. This frequency band is chosen as there are no licensing issues in this band and higher frequency allows the use of a smaller antenna. After validating the simulations with measurements in human muscle tissue, simulations are extended over a broad range of ε_r and σ representing various homogeneous human tissues to calculate and model the PL. The PL that way obtained is used to propose a PL model applicable for the various homogeneous tissues in a human body.

2. Configurations
2.1. Homogeneous human tissues

Wave propagation is first investigated at 2.457 GHz in human muscle tissue (ε_r =50.8 and σ = 2.01 S/m [1]) using measurements and simulations for insulated dipoles. Two identical insulated dipoles of length, l = 3.9 cm are developed for measurements where the dipole arms are perfect electric conductors (PEC) surrounded with an insulation made of polytetrafluoroethylene ε_r = 2.07 and σ = 0 S/m for a frequency of 2.457 GHz. The dipole arms have a diameter t_1=1 mm and the diameter of the insulation is t_2=5 mm.

Measurements are executed using a vector network analyzer NWA (Rohde & Schwarz ZVR) and the scattering parameters $|S_{11}|_{dB}$ and $|S_{21}|_{dB}$ (with respect to 50Ω) between Tx and Rx for the different separations are determined. A flat phantom, representing the trunk of a human body and recommended by CENELEC standard EN50383 [2] (dimensions 80x50x20 cm^3), is filled with muscle tissue simulating fluid (ε_r = 50.8 and σ =2.01 S/m at 2.45 GHz [1]). The insulated dipole antenna is connected to the NWA using a coaxial cable. The two insulated dipoles are immersed, placed parallel and lined up for maximal power transfer at 5 cm above the bottom of the flat phantom. The measurements are performed every 2 mm starting from distances of 6 mm up to 8 cm.
Simulations are performed using a 3D electromagnetic solver SEMCAD-X (SPEAG, Switzerland), a finite-difference time-domain (FDTD) program and FEKO (EMSS, South Africa), a method of moments (MoM) program. SEMCAD-X enables non-uniform gridding. The maximum grid step in the muscle tissue medium is 1 mm at 2.457 GHz. For accurate modeling in the MoM tool, segmentation rules are adhered to (segment length= λ/12, edge length = λ/12, where λ = wavelength in muscle tissue medium). In both simulations a voltage source is used, which is placed in the gap between the two dipole arms. To determine the influence of ε_r and σ on PL, further PL simulations are carried out using the insulated dipole antenna for a range of ε_r and σ values. ε_r is varied from $5 \leq \varepsilon_r \leq 65$ and σ from $0.5 \text{ S/m} \leq \sigma \leq 3.5$ S/m as most human tissues at 2.45 GHz are characterized by an ε_r and σ in this range [3]. The simulations of the combination of ε_r and σ are carried out from 6 mm up to a distance of 8 cm using the MoM program. MoM program is used as its

978-1-4244-6051-9/11/$26.00 ©2011 IEEE

simulations are faster than the FDTD program and a total of 1547 simulations were carried out for PL as a function of distance d, σ, and ε_r.

2.2 Heterogeneous medium

PL in heterogeneous medium is investigated using an enhanced anatomical model of a 6 year male child from the *Virtual Family* [VFM]. The model is based on magnetic resonance images (MRI) of healthy volunteers. The male child model (virtual family boy, VFB) has a height of 1.17 m and a weight of 19.5 kg. The model consists of 81 different tissues. We select the male child model as capsule endoscopy is used as a tool for diagnosis for children with evidence of internal bleeding and abdominal pain. The dielectric properties of the body tissues have been taken from the Gabriel database [3]. Simulations to determine PL are carried out using FDTD technique in SEMCAD-X. Insulated dipole antennas are placed in the trunk of the male child model to determine PL from a distance of 6 mm up to 120 mm.

3. Results
3.1 PL in human muscle tissue

PL is defined as the ratio of input power at port 1(P_{in}) to power received at port 2 (P_{rec}) in a two-port setup. PL in terms of transmission coefficient is defined as $1/|S_{21}|^2$ with respect to 50 Ω when the generator at the Tx has an output impedance of 50 Ω and the Rx is terminated with 50 Ω This allows us to regard the setup as a two-port circuit for which we determine $|S_{21}|_{dB}$ with reference impedances of 50 Ω at both ports. Fig.1 (a) shows the simulated and measured PL in human muscle tissue as a function of distance *d* for the insulated dipole. The measured and the simulated values show excellent agreement up to 8 cm. The deviations between the measurements and the simulations are very low: with SEMCAD-X, the maximal and average deviation up to 8 cm are 1.7 dB and 0.8 dB, respectively, and for FEKO the maximal and average deviation are 3.4 dB and 1.3 dB, respectively. Now, the measurement results are used to develop a PL model (see Fig. 1(a)) as a function of distance in human muscle tissue at 2.457 GHz which is as follows:

$$PL|_{dB} = (10 \log_{10} e^2)\, \alpha_1 d + C_1|_{dB} \quad for\ (d \le d_{bp}), \tag{1}$$
$$PL|_{dB} = (10 \log_{10} e^2)\, \alpha_2 d + C_2|_{dB} \quad for\ (d \ge d_{bp}), \tag{2}$$

where the parameters α_1 and α_2 are the attenuation constants [1/cm], $C_1|_{dB}$ and $C_2|_{dB}$ are constants, d_{bp}= 2.78 cm is the breakpoint where the mutual coupling between the transmitter and the receiver ends, and *d* is in cm. The model consists of two regions: *Region 1* and *Region 2*. *Region 1*($d \le d_{bp}$) extends from 0 cm to 2.78 cm from the Tx antenna and is the region where the Tx and the Rx antennas interact with each other due to mutual coupling which alters the impedance of the Tx antenna. *Region 2*, ($d \ge d_{bp}$) extends from 2.78 cm and beyond. The parameter values in (1) and (2) are obtained by using a least square-error method and are shown in Table 1.

3.2 PL in different human tissues

PL as a function of distance for a range of σ (0.5 S/m ≤ σ ≤ 3.5 S/m) and ε_r ($5 \le \varepsilon_r \le 65$), at frequency of 2.45 GHz is discussed in this section. As conductivity introduces losses, PL increases with increasing conductivity as shown in Fig. 1(b), while PL decreases with increasing permittivity. We discuss the dependency of the attenuation constant α on ε_r which will help us further in understanding the decrease in PL with increase in ε_r. Using the PL model of (1) and (2) we obtain the attenuation constants α_1, α_2, the constants $C_1|_{dB}$, $C_2|_{dB}$, and d_{bp} for the range of the dielectric parameters. The obtained values are used to derive models and these models are put in (1) and (2) to obtain (3) and (4). Thus a PL model as a function of d, ε_r, and σ at 2.457 GHz is obtained.

$$PL|_{dB} = (10 \log_{10} e^2)\, (A_1 e^{(\varepsilon_r B_1)} + D_1) \cdot (E_1 \sigma + F_1)\, d + (U_1 e^{(V_1/\varepsilon_r)} + W_1) \cdot (X_1 \sigma + Y_1) \quad for\ (d \le d_{bp}), \tag{3}$$
$$PL|_{dB} = (10 \log_{10} e^2)\, (A_2 e^{(\varepsilon_r B_2)} + D_2) \cdot (E_2 \sigma + F_2)\, d + (U_2 e^{(V_2/\varepsilon_r)} + W_2) \cdot (X_2 \sigma + Y_2) \quad for\ (d \ge d_{bp}), \tag{4}$$

From (3) and (4) it is observed that the attenuation constants α_1 and α_2 increase with increasing value of σ and decrease with an increasing value of ε_r. Hence PL increases for higher σ and decreases for higher ε_r. This can be explained as follows, for plane waves [5] the attenuation constant α in a lossy medium is directly proportional to the conductivity of a medium (thus PL increases for higher σ) and is inversely proportional to the square root of the permittivity (thus PL decreases for higher ε_r). A similar trend is found in the results obtained here. The value of the parameters in the attenuation constant model, A_1, A_2, B_1, B_2, E_1, E_2, F_1, and F_2 are provided in the Table I. The constants C_1 and C_2 increase with an increase in ε_r and decrease with an increase in σ. The value of the parameters in the constant C_1 and C_2 models U_1,

U_2, V_1, V_2, W_1, W_2, X_1, X_2, Y_1, and Y_2 are provided in the Table I. The break point is also deduced for the PL model for the combinations of ε_r and σ. It is seen that d_{bp} decreases as σ increases. As σ increases, higher losses are introduced due to which the coupling only exists for smaller distances, hence d_{bp} decreases. We observe that d_{bp} increases with increase in ε_r. As the PL decreases with an increase in ε_r we can deduce that at higher ε_r coupling exists over a larger distance between the transmitting and the receiving antenna. We develop a model for the d_{bp} as a function of ε_r and σ and the parameter values for P, Q, R S and T are provided in Table 1.

$$d_{bp}(\varepsilon_r, \sigma) = (Pe^{(Q\,\varepsilon_r)}) \cdot (Re^{-(S\sigma)} + T) \tag{5}$$

We validate the models (3) and (4) by comparing them with the PL obtained in the simulation. The mean deviation from the models is only 0.83 dB and the maximum mean deviation is 2.56 dB for the entire range of permittivity and conductivity with a total combination of 1547 simulations, which is very good.

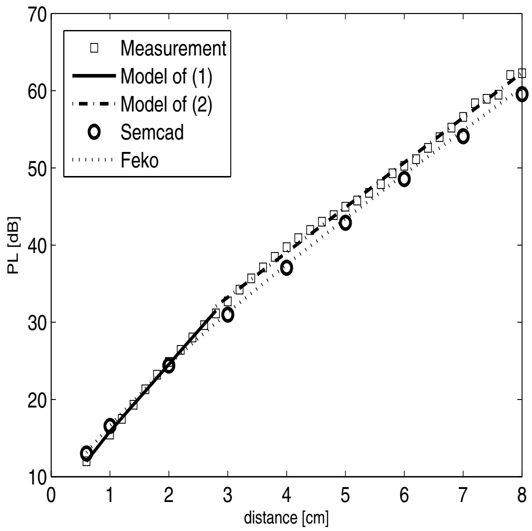

Fig: 1(a) Measured, simulated PL, and fitted models as a function of separation between the Tx and Rx

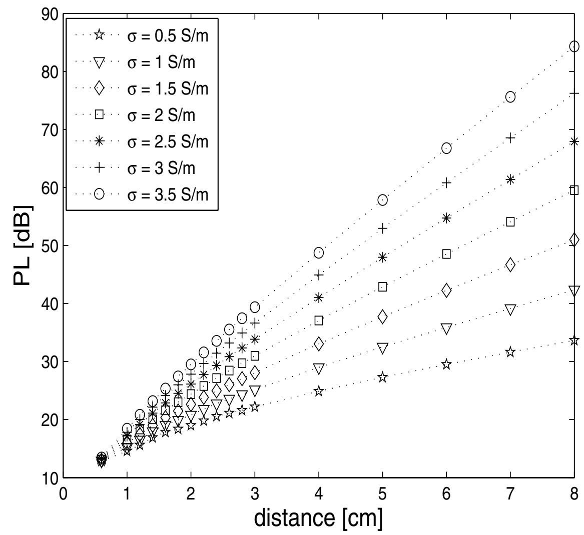

Fig: 1(b) Path loss vs. separation between the Tx and the Rx for σ (ε_r = 50).

3.3 PL in Heterogeneous Model

Fig. 2 shows PL in the heterogeneous medium with a separation between the insulated dipole antennas up to 12 cm and the comparison with the PL in homogeneous medium having dielectric properties of the liver and stomach. PL of the heterogeneous medium shows a slight change in slope at distances where the Rx antenna makes a transition from one medium to the other (at 5 cm) in Fig. 2 which is due to change in the dielectric property of the tissues and thus due to the difference in the attenuation constant for each tissue through which the antenna traverses. PL in heterogeneous medium from a distance of 0.6 cm to 4 cm is in the stomach and hence it is compared to the PL in homogeneous medium with dielectric property of the stomach (ε_r = 62.16 and σ = 2.21 S/m): it can be observed that the PL of both are similar and follow the same trend. The PL in heterogeneous medium from 5 cm to 12 cm (in Fig. 2) is in the liver and hence it is compared to the PL in homogeneous medium with dielectric properties (ε_r = 54.81 and σ = 2.25 S/m) which also shows the same trend. In Fig. 2 PL in heterogeneous human model is in between the PL of the homogeneous tissues and lower than the PL in worst-case realistic tissue which is the small intestine (ε_r = 54.42 and σ = 3.17 S/m). The deviation between the PL in heterogeneous human model and homogeneous human tissues can be attributed to various parameters in the heterogeneous medium for e.g., proximity of different tissue layers, and the transition of the whole antenna to another tissue does not take place immediately but the antenna moves into the next tissue part by part.

4. Conclusion

We investigated the influence of ε_r and σ of the various tissues on the PL thus providing a better understanding of PL in different tissues. An extensive PL study has been performed using insulated dipoles within various homogeneous lossy human tissues and an empirical PL model is developed that describes the relationships between the PL and the relative permittivity ε_r the conductivity σ of the human tissues, and the distance between the antennas at 2.457 GHz. The PL in homogeneous medium is also compared with the PL in heterogeneous medium.

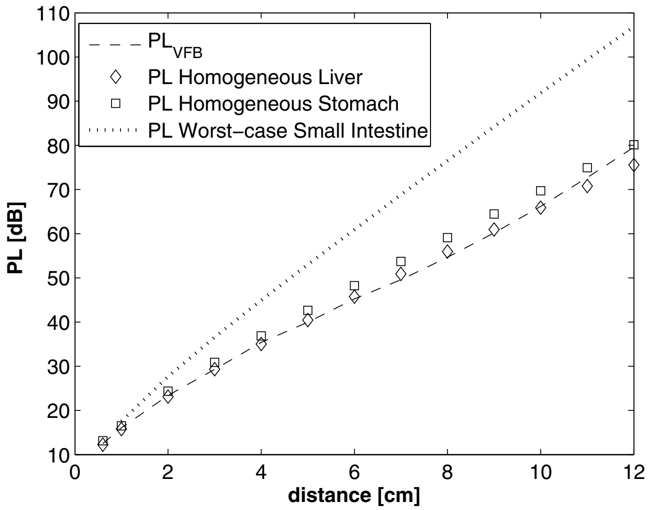

Figure 2: PL in the VFB and in homogeneous medium of stomach and liver and PL for worst tissue property.

Table 1: Parameter values of the PL model

Parameter	**α_i [1/cm]**	**C_i [dB]**	**S D[dB]**	**dev_{imax}[dB]**	**dev_{iavg}[dB]**	
Model of (1)	0.99	7.18	0.15	0.56	0.26	
Model of (2)	0.66	15.79	0.28	1.22	0.40	
	A_i	**B_i**	**D_i**	**E_i**	**F_i**	**Relative Error**
Model of α_1 in (3)	7.19	-0.04	4.86	0.05	0.05	3.9%
Model of α_2 in (4)	3.02	-0.04	1.83	0.11	0.07	3.5%
	U_i	**V_i**	**W_i**	**X_i**	**Y_i**	
Model of C_1 in (3)	1.98	-22.11	0.66	-1.05	6.56	0.52 dB
Model of C_2 in (4)	0.47	-28.59	0.55	-2.24	21.18	0.33 dB
	P_i	**Q_i**	**R_i**	**S_i**	**T_i**	
Model of d_{bp} in (5)	0.29	0.01	4.83	0.30	0.68	7.3%

7. References

1. FCC OET Bulletin 65, Revised Supplement C, “Evaluating Compliance with FCC Guidelines for Human Exposure to Radiofrequency Electromagnetic Fields,” *Federal Communication Commission*, Office of Engineering and Technology, June 2001.

2. CENELEC EN50383, “Basic standard for the calculation and measurement of electromagnetic field strength and SAR related to human exposure from radio base stations and fixed terminal stations for wireless telecommunication systems (110 MHz - 40 GHz),” Sept 2002.

3. C. Gabriel and S. Gabriel., “Compilation of the dielectric properties of body tissues at RF and microwave frequencies,” *[ONLINE] Available: http://www.brooks.af.mil/AFRL/HED/hedr/reports/dielectric/home.html. Tech. Rep. AL/OE-RE-1996-0037,* 1996.

4. D. Kurup, W. Joseph, G. Vermeeren, and L. Martens, “Path loss model for in-body communication in homogeneous human muscle tissue,” *IET Electronics Letters*, pp. 453–454, April 2009.

5. J. A. Stratton, *Electromagnetic Theory, First Edition* McGraw-Hill Book Company Inc., 1941, pp.276-277.